UNIVERSITÀ DI SIENA 1240

USiena

New bio-magnetostratigraphic data on the Miocene Moria section (Northern Apennines, Italy): connections between the Mediterranean region and the North Atlantic Ocean

This is a pre print version of the following article:

Original:

Di Stefano, A., Baldassini, N., Maniscalco, R., Speranza, F., Maffione, M., Cascella, A., et al. (2015). New bio-magnetostratigraphic data on the Miocene Moria section (Northern Apennines, Italy): connections between the Mediterranean region and the North Atlantic Ocean. NEWSLETTERS ON STRATIGRAPHY, 48(2), 135-152 [10.1127/nos/2015/0057].

Availability:

This version is availablehttp://hdl.handle.net/11365/990263 since 2021-03-25T18:18:10Z

Published:

DOI: http://doi.org/10.1127/nos/2015/0057

Terms of use:

Open Access

The terms and conditions for the reuse of this version of the manuscript are specified in the publishing policy. Works made available under a Creative Commons license can be used according to the terms and conditions of said license.
For all terms of use and more information see the publisher's website.

(Article begins on next page)

13 November 2026

Newsletters on Stratigraphy
Published online January 2015

PrePub Article

New bio-magnetostratigraphic data on the Miocene Moria section (Northern Apennines, Italy): connections between the Mediterranean region and the North Atlantic Ocean

Agata Di Stefano[1], Niccolò Baldassini[1]*, Rosanna Maniscalco[1], Fabio Speranza[2], Marco Maffione[3], Antonio Cascella[4], and Luca Maria Foresi[5]

With 8 figures and 3 tables

Abstract. New bio-magnetostratigraphic data have been acquired from the Burdigalian part of the Moria section in the Umbria–Marche Apennine (Central Italy). The investigated sedimentary sequence is 55 meters thick and comprises the transition between the Bisciaro and the Schlier formations (*Auctorum*), composed of five meters of indurated marly limestones, followed by about 40 meters of blue marly clays capped by 10 m of alternating clays and calcareous layers. According to existing literature, the sequence contains the so-called "Piero della Francesca Level" (*Auctorum*), a few-centimeters-thick biotite-rich level. The sequence has been sampled for paleomagnetic and calcareous plankton analyses. Four magnetic polarity zones have been documented in the middle and upper part of the section. The calcareous plankton content shows different degrees of preservation, from poor to good for calcareous nannofossils and poor to medium for planktonic foraminifers. Several useful biohorizons have been observed and chronologically constrained through calibration to the magnetostratigraphic data.

The studied section ranges from the top of Chron C5Dr.1n to Chron C5Cn.2r, covering the time interval from 17.7 to 16.4 Ma (according to the ATNTS04) almost continuously, with a small hiatus of at least 34 ka at the C5Dn/C5Cr transition. The integration of our results with those from previous studies of the same section and comparisons with data from other Mediterranean and North Atlantic sequences allows to evaluate the synchrony of the observed biohorizons with other parts of the Mediterranean and the Atlantic Ocean during a still relatively poorly known time interval.

Key words. Miocene, calcareous plankton biostratigraphy, magnetostratigraphy, Mediterranean, North Atlantic

Authors' addresses:

[1] Dipartimento di Scienze Biologiche, Geologiche e Ambientali, Sezione di Scienze della Terra, Università di Catania, Corso Italia 57, 95129, Catania, Italy. E-Mail: distefan@unict.it, nbaldas@unict.it, maniscal@unict.it

[*] Corresponding author; E-Mail: nbaldas@unict.it

[2] Istituto Nazionale di Geofisica e Vulcanologia, Via di Vigna Murata 605, 00143, Roma, Italy. E-Mail: fabio.speranza@ingv.it

[3] Paleomagnetic Laboratory "Fort Hoofddijk", Department of Earth Science, Utrecht University, Budapestlaan 17, 3584 CD Utrecht, The Netherlands. E-Mail: m.maffione@uu.nl

[4] Istituto Nazionale di Geofisica e Vulcanologia, Via della Faggiola 32, 56126, Pisa, Italy. E-Mail: cascella@ingv.it

[5] Dipartimento di Scienze Fisiche, della Terra e dell'Ambiente, Sezione di Scienze della Terra, Università di Siena, Via Laterina 8, 53100, Siena, Italy. E-Mail: luca.foresi@unisi.it

© 2015 Gebrüder Borntraeger, Stuttgart, Germany
www.borntraeger-cramer.de
DOI: 10.1127/nos/2015/0057
0078-0421/2015/0057 $ 4.50

uncorrected proofs

1. Introduction

The Moria section in the Umbro–Marche Apennine of Central Italy represents a well-known lower–middle Miocene sedimentary sequence in the Mediterranean region (Fig. 1). The section has been subject to detailed integrated stratigraphic studies over the past two decades because of the favorable exposure, the presence of abundant calcareous plankton and the presence of radiometrically datable layers (Fornaciari and Rio 1996, Fornaciari et al. 1996, Deino et al. 1997, Di Stefano et al. 2008). A detailed lithostratigraphy has been presented by Deino et al. (1997), who published an integrated bio-magnetostratigraphic study (Fig. 2) for the ca. 100 m thick succession. However, reliable paleomagnetic directions are limited and discontinuous throughout the studied section. In this study we re-examined the lower, 55-m-thick portion of the section coinciding with the lower part of the section reported by Deino et al. (1997) (Figs. 2, 3), namely the segment encompassing the Bisciaro/Schlier transition.

The interpretation of the observed magnetozones was made through tie-points provided by main calcareous plankton horizons. Furthermore, a number of additional plankton events were detected and magnetostratigraphically constrained. The obtained data were integrated with those gathered previously by Di Stefano et al. (2008), and compared with other Mediterranean sections and with North Atlantic DSDP Hole 608 (Ruddiman et al. 1987, Miller et al. 1991, Olaffson 1991, Gartner 1992, Di Stefano et al. 2011a). This resulted in an improved stratigraphic resolution for the interval ranging from the base of Chron C6n (19.7 Ma) to Chron C5ADr (14.7 Ma), and the establishment of correlations between the Mediterranean region and the North Atlantic Ocean across the lower–middle Miocene boundary.

2. Geological setting

The Moria section (base: 43° 30.176′ N, 12° 35.619′ E; top: 43° 30.151′ N, 12° 35.533′ E) crops out in the Umbria–Marche Apennines of Central Italy, along the road connecting the villages of Palcano and Moria, on the west side of Mount Petrano in the Marche Region (Figs. 1, 3). The section includes the uppermost part of the Bisciaro Formation (Fm) and most of the Schlier Fm, which represent the lower–middle Miocene deposits of the Umbria–Marche succession (Capuano 2009).

The Umbria–Marche succession was deposited in a pelagic environment from the early Jurassic to the early Cretaceous, within an extensional tectonic regime linked to the Tethyan rifting phase, followed by hemipelagic deposition within a sector that connected the flexured foreland and the foredeep. Thus, during the late Cretaceous to early Oligocene, the calcareous

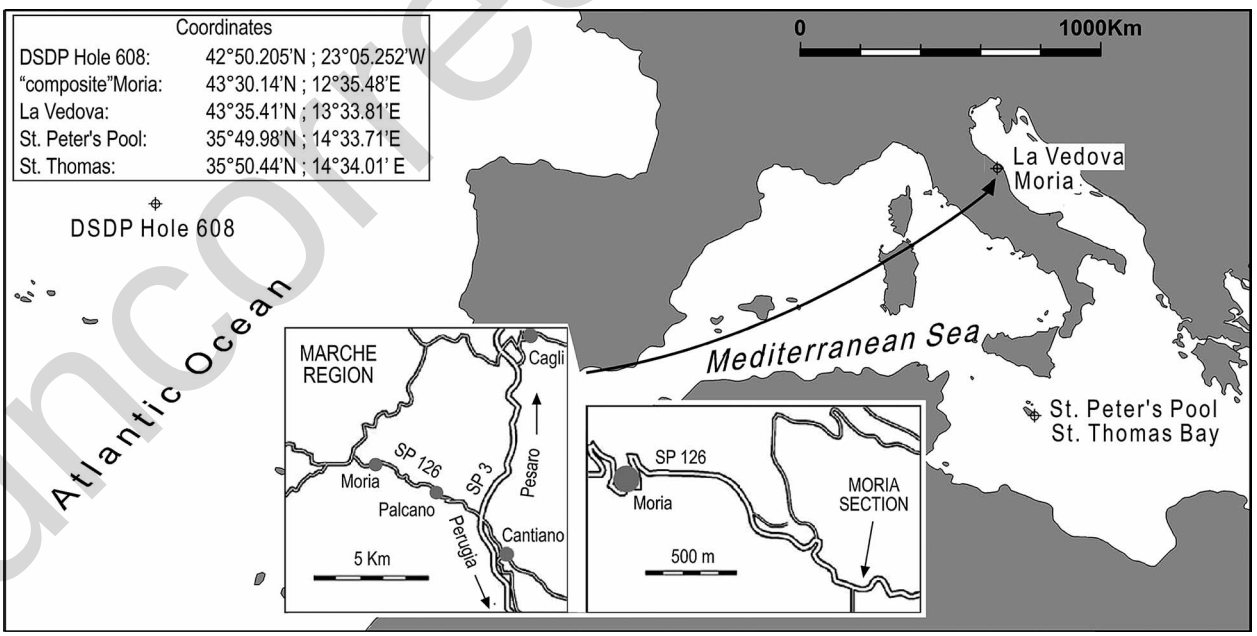

Fig. 1. Location map of the Moria section and of the other sections considered in the text.

Uncorrected Proofs

Maiolica, Marne a Fucoidi, Scaglia Bianca, and Scaglia Rossa formations were deposited in the Umbria–Marche basin (Capuano 2009, Guerrera et al. 2012). After the late Oligocene, the complex geodynamic setting of the Apennine orogenesis was recorded in the deposition of the Scaglia Variegata and Scaglia Cinerea formations, and subsequently in Miocene sediments characterized by a progressive reduction of the carbonaceous fraction and the increase of fine clastic material (Guerrera et al. 2012), which gave rise to the Bisciaro, Schlier and Marnoso-Arenacea formations.

The Bisciaro Fm consists of marls and siliceous marly limestones that are finely layered, and gray and greenish-gray in color (ocher if altered), with a progressive upward increase of the terrigenous fraction. Blackish-gray cherty lists and nodules are locally present in the lower and middle part of the formation. The Bisciaro Fm is characterized by frequent volcanic ashes, tuffites and bentonites resulting from syn-tectonic volcanic activity. The well-known "Raffaello Bed" (Coccioni and Montanari 1994) dated at about 22 Ma traditionally marks the Scaglia Cinerea/Bisciaro lithostratigraphic boundary.

The Bisciaro-Schlier transition is gradual and not always well defined. Coccioni and Montanari (1992) identified the boundary between the two formations in a 10–15 cm thick biotite-rich layer referred to as "Piero della Francesca Level", radiometrically ($^{40}Ar/^{39}Ar$) dated at 17.1 ± 0.16 Ma (Deino et al. 1997). However, more recent interpretations place the boundary in correspondence with a significant reduction (or disappearance) of the calcareous and volcaniclastic layers (Capuano 2009, Guerrera et al. 2012).

The turbidite-type Schlier Fm is characterized by a sedimentation rate of ca. 40 m/Ma (Capuano 2009). Subdivided into a lower and an upper marly member, it consists mainly of marls and clayey marls. An intermediate member is composed of alternating marls/clayey marls and carbonate-rich layers. The upper boundary to the Marnoso Arenacea Fm is traditionally placed at the level of the first arenaceous horizon (Capuano 2009).

3. Previous studies and description of the Moria section

The stratigraphy of the Moria section has been described previously by Fornaciari et al. (1996), Fornaciari and Rio (1996), and Deino et al. (1997) (Figs. 2, 3). The lower part of the 100 m thick section consists of few meters of indurated gray/beige limestones, a short interval of alternating soft marls and carbonates, and about 30 meters of gray/green marls. The upper part is represented by 40 m of alternating marls and clayey marls interlayered with whitish indurated calcareous layers, capped by marl. Deino et al. (1997) reported the "Piero della Francesca Level" at about 20 m above the base of the section. Biostratigraphically, the section falls within the planktonic foraminifer zones N6 (top) to N8 of Blow (1969) (mainly corresponding to the *G. trilobus – P. glomerosa* s.l. zones of Iaccarino and Salvatorini 1982 and Iaccarino 1985) and the calcareous nannofossil zones MNN3b–MNN5a (Fornaciari and Rio 1996, Fornaciari et al. 1996) straddling the Burdigalian-Langhian boundary.

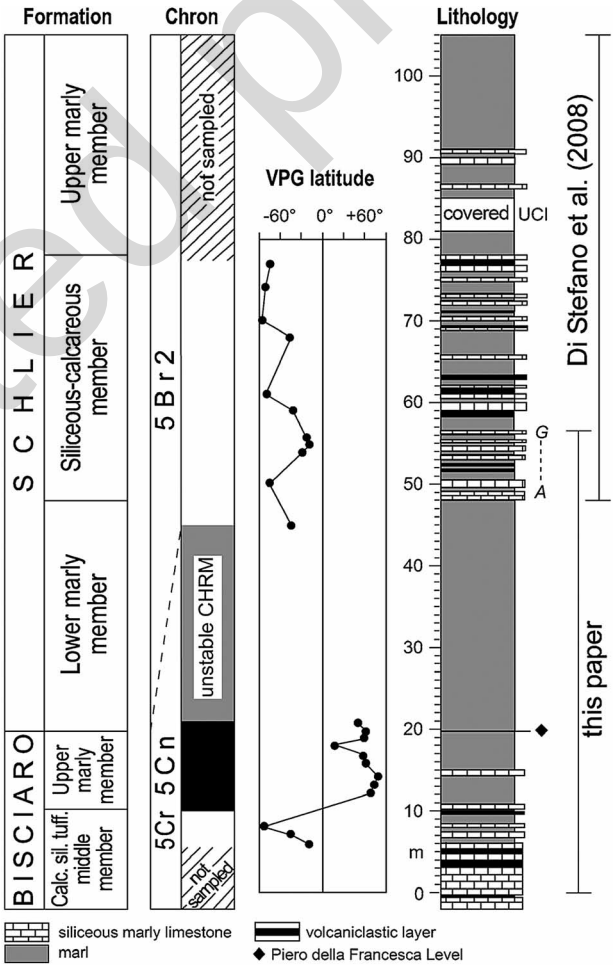

Fig. 2. Lithostratigraphic log and paleomagnetic data of the Moria section, redrawn after Deino et al. (1997). The part considered in the present study and the part examined by Di Stefano et al. (2008) are indicated. The letters refer to the limestone layers as reported in Figs. 3 and 4. UCI = Upper Covered Interval.

uncorrected proofs

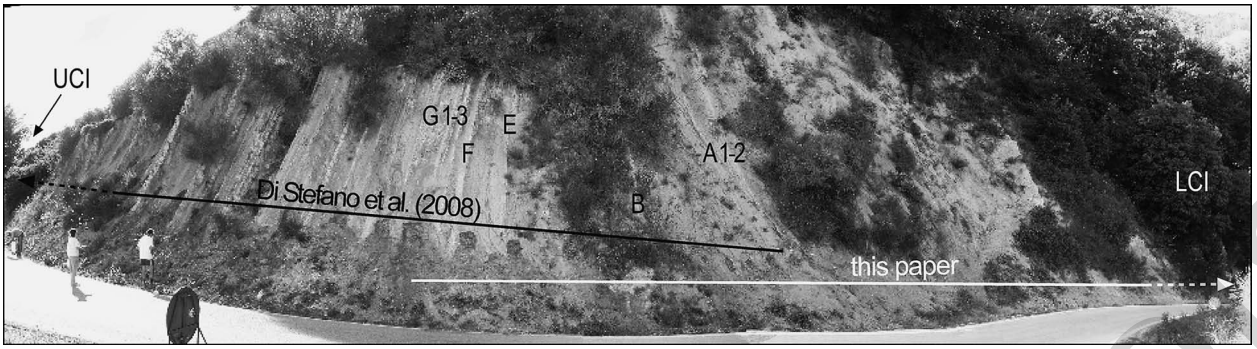

Fig. 3. Panoramic view of the composite Moria section. The part considered in the present study and the one examined by Di Stefano et al. (2008) are indicated. LCI = Lower Covered Interval; UCI = Upper Covered Interval. The letters refer to the limestone layers as reported in Figs. 2 and 4.

The earliest magnetostratigraphic study could resolve magnetization directions in 23 samples (Deino et al. 1997) (Fig. 2), suggesting the presence of a 4-m-thick reversed polarity interval at the base of the section that was interpreted as Chron C5Cr based on the comparison with the Contessa section (Montanari et al. 1997). A normal polarity zone extending for about 11 meters follows, interpreted as Chron C5Cn (Deino et al. 1997). No reliable paleomagnetic data were acquired from the middle part of the section. An interval of reversed polarity was observed in the intermediate member of the Schlier Fm, interpreted to represent Chron C5Br2 (Deino et al. 1997). It must be noted that this interpretation is not consistent with the radiometric age of the "Piero della Francesca Level" reported by the same authors (17.1 ± 0.16 Ma), as the C5B/C5C boundary, which should be very close to it (Fig. 2), has an age of 15.97 Ma (Lourens et al. 2004).

A high-resolution calcareous plankton biostratigraphy of the upper part of the section (encompassing the uppermost layers of the lower marly, the siliceous-calcareous and the upper marly members of the Schlier Fm; Fig. 2) was recently published by Di Stefano et al. (2008). Unfortunately, no magnetostratigraphic age control could be provided for this interval. The calcareous plankton events recognized by Di Stefano et al. (2008) can now be chronologically constrained through the comparison with the subsequent study of Turco et al. (2011) who detected and dated the same bioevents at the La Vedova section, about 80 km east of the Moria section, along the Conero Riviera (Marche region, Central Italy; Fig. 1).

In this study, the lower 55 m of the Moria section have been re-sampled for bio-magnetostratigraphic analysis (Figs. 4, 5, 6), starting from the limestones of the Bisciaro Fm and recognizing the "Piero della Francesca Level", 22 m from the base of the section. Minor differences with respect to the description reported by Deino et al. (1997), for instance the different position of the "Piero della Francesca" layer, are due to the presence of a 4-m-thick vegetation-covered interval in the basal part of the section (LCI in Fig. 3). The top of the studied section, characterized by thin calcareous layers within prevailing clays of the Schlier Fm, overlaps the basal part of the section studied by Di Stefano et al. (2008) (Figs. 2, 3).

4. Methodology

Sixty-nine samples were considered for qualitative and semiquantitative analyses of planktonic foraminifers. Samples were washed through a 63 μm sieve. Some encrusted specimens of biostratigraphically significant taxa were cleaned by ultrasonic bathing to allow better observation of diagnostic characters. Sixty-eight smear slides for calcareous nannofossil analyses were prepared and studied using standard methods (Haq and Lohman 1976, Rio et al. 1990), including analysis under a 1000x magnification polarized microscope (transmitted light and crossed nicols). Following Rio et al. (1990) and Fornaciari et al. (1996), the relative abundances of all species within the genera *Sphenolithus* and *Helicosphaera* were determined by counting 30 and 50 specimens, respectively.

Sixty paleomagnetic cores were drilled using a petrol-powered portable drill cooled by water, and oriented in situ using a magnetic compass corrected for the local magnetic declination for the year 2009 (ca. 2°). Afterwards, the cores were cut into standard paleomagnetic specimens of 22 mm height. Paleomagnetic measurements were performed at the Istituto Nazio-

Uncorrected Proofs

nale di Geofisica e Vulcanologia (INGV Rome, Italy). Natural remanent magnetization (NRM) of the specimens was measured in a magnetically shielded room with a DC-SQUID cryogenic magnetometer (2G Enterprises, USA). Demagnetization diagrams were obtained through a stepwise (25 °C increments) thermal cleaning treatment carried out in a magnetically shielded oven up to complete demagnetization of the samples. Demagnetization data were then plotted on orthogonal demagnetization diagrams (Zijderveld 1967), and the magnetization components were isolated by principal component analysis (Kirschvink 1980) according to standard paleomagnetic procedures.

5. Magnetostratigraphy

Magnetization of the analyzed samples is very weak and ranges between 17 and 293 μA/m (mean value = 58 μA/m), denoting a very low concentration of the magnetic minerals. Being close to the instrumental sensitivity of the magnetometer (~5 μA/m), only 28 out of 60 samples yielded stable and interpretable demagnetization diagrams (Figs. 4, 5a). Most of the samples are characterized by two components of magnetization (Fig. 5a). The low-stability component, possibly resulting from a present-day geomagnetic field overprint, was removed at 100–120 °C (denoting possible presence of goethite). The high-stability component was in general isolated between 120 and 300 °C, pointing to iron sulphides (likely greigite) as the main magnetic carrier.

Demagnetization experiments were not continued above 300 °C due to the occurrence of mineralogical transformation upon heating (i.e., iron sulphides transformed into magnetite) that resulted in a spurious increase of magnetic susceptibility and magnetization. Nevertheless, although this process inhibited complete removal of the high-stability components, in the demagnetization diagrams (Fig. 5a) they clearly decay towards the origin of the axes (typical feature of high-stability components of magnetization).

The most commonly used approaches to test the reliability of the isolated remanence directions in paleomagnetic studies (primary vs. secondary magnetization) are the reversal test (McFadden and McElhinny 1990), and the fold test (McFadden 1990). A positive result of the reversal test provides evidence that magnetic remanence was acquired over a longer time interval during which at least one geomagnetic reversal occurred, excluding in this way that a rapid remagnetization event occurred since the deposition of the sediment. Out of 28 isolated directions, 14 have a reversed polarity and 14 a normal polarity (Figs. 4, 5b). Their distribution is, at a first glance, somewhat antipodal, supporting the possibility of a positive reversal test. However, likely due to the low intensity of the magnetizations, which resulted into a larger scatter of the paleomagnetic directions, the performed reversal test provided an undetermined result (note this is not a negative reversal test). On the other hand, the entire section displays a quite homogenous bedding attitude of 214°/63° (dip direction/dip), implying that the statistical parameters associated with the distribution of the isolated high-stability components (i.e., k and α_{95}) are identical before and after bedding correction, hence inhibiting any meaningful fold test.

When converted to normal polarity state, the isolated directions (N = 28) after bedding correction display

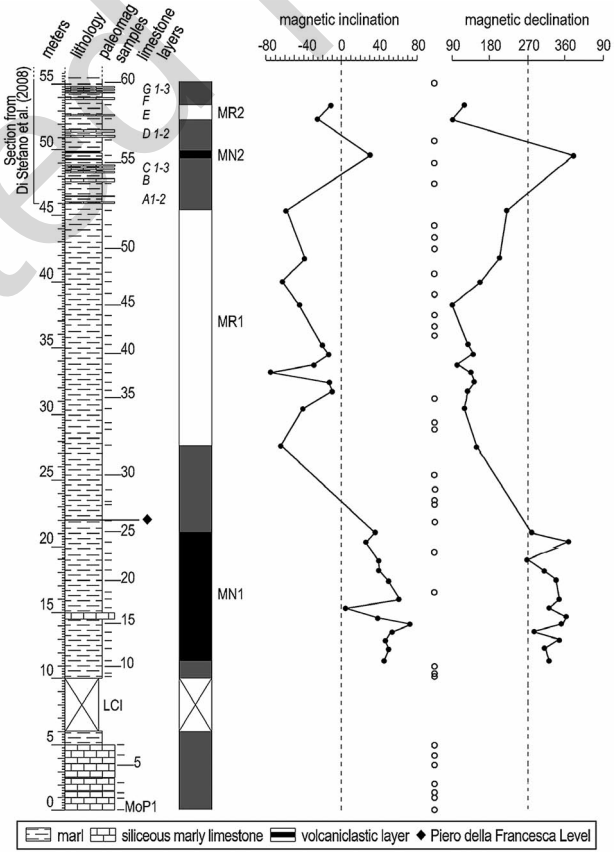

Fig. 4. Lithological log of the succession investigated in the present study; sample positions are indicated on the right. The black, white and gray intervals in the polarity record represent normal, reversal and uncertain polarity intervals, respectively. The empty circles represent samples that were not interpreted. LCI = Lower Covered Interval.

Uncorrected proofs

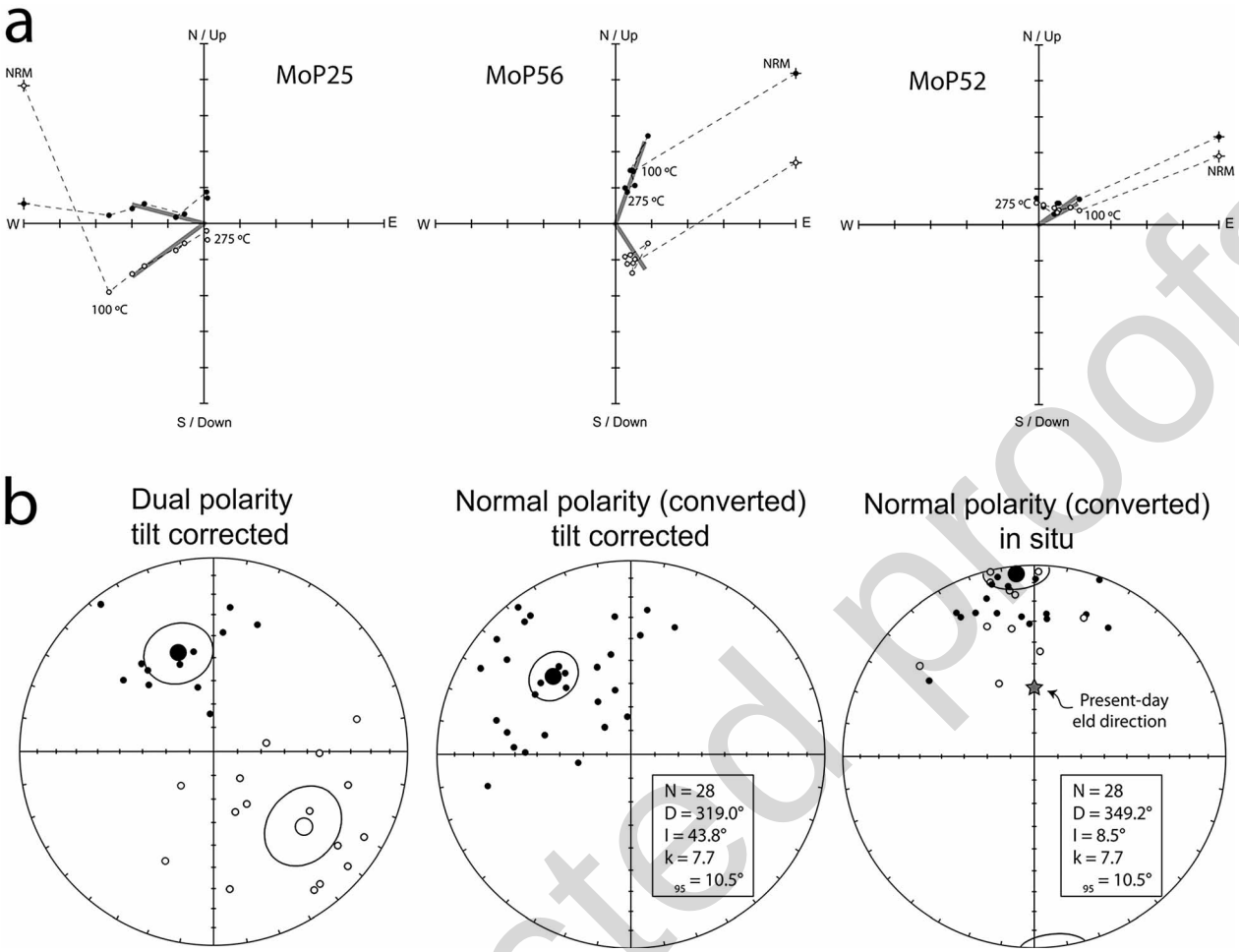

Fig. 5. **a** – Zijderveld diagrams (Zijderveld 1967) of three representative samples showing normal (samples MoP25 and MoP56) and reverse (sample MoP52) polarity of magnetisation (tilt-corrected coordinates). Solid and open dots indicate projections on the horizontal and vertical planes, respectively. Demagnetization step values in °C are shown, together with the interval that was used to isolate the characteristic remanent magnetisation (thick grey line). **b** – Magnetic component analysis and graphic output were carried out with REMASOFT 3.0 software [Chadima and Hrouda, 2006].

a well-clustered distribution with declination (D) = 319.0°, inclination (I) = 43.8°, and statistical Fisherian (Fisher 1953) parameters k = 7.7, and $\alpha 95 = 10.5°$ (Fig. 4). Before bedding correction (in situ), the mean value (D = 349.2°, I = 8.5°) is clearly different from the direction of the present-day geomagnetic field (Fig. 5b), hence a recent magnetic overprint can be firmly excluded. Furthermore, the computed mean direction for the Moria section is consistent with the moderate (few tens of degrees) counterclockwise rotations characterizing coeval rocks from adjacent sectors of the northern Apennines (Speranza et al. 1997). This provides strong evidence for the primary origin of the isolated directions. Accordingly, the obtained paleomagnetic data are reliable and will be used in the following magnetostratigraphic reconstruction.

The distribution of the magnetic polarities within the Moria section resulting from this study (Fig. 4, Table 1) indicates the presence of four magnetozones, from bottom to top: MN1 = normal polarity interval (samples MoP11–MoP25), MR1 = reversed polarity interval (samples MoP31–MoP53), MN2 = normal polarity interval (sample MoP56), and MR2 = reversed polarity interval (samples MoP58–MoP59).

6. Biostratigraphy

6.1 Planktonic foraminifers

Planktonic foraminifers are generally abundant throughout the investigated part of the Moria section, but poorly to medium preserved in samples from the calcare-

Uncorrected proofs

ous strata of the Bisciaro Fm. The poor preservation due to encrustation and carbonate dissolution increases the portion of dissolution-resistant taxa within the assemblages, thus altering the original abundance pattern. The preservation of planktonic foraminifers improves upwards in the marls of the Schlier Fm. However, recrystallized, broken and mechanically deformed tests are common throughout the section.

The assemblages are dominated by *Dentoglobigerina* spp., *Globigerina praebulloides*, *Globigerinoides quadrilobatus* group, *Globorotalia praescitula*, and *Paragloborotalia acrostoma* (Fig. 6). Less abundant taxa include *Globigerinoides altiaperturus*, *G. diminutus*, *G. subquadratus*, *Globoquadrina dehiscens*, *Globoturborotalita druryi*, *G. woodi*, and the *Tenuitellinata angustiumbilicata* group. Finally, *Catapsydrax dissimilis*, *Paragloborotalia bella*, *P. siakensis*, and *Turborotalita quinqueloba* show rare and scattered occurrences.

The generally poor preservation of the assemblages hampered the application of quantitative approaches, and only semiquantitative distributions of selected taxa are reported (Fig. 6). The ranges and occurrence characteristics of the most significant taxa are discussed in the following.

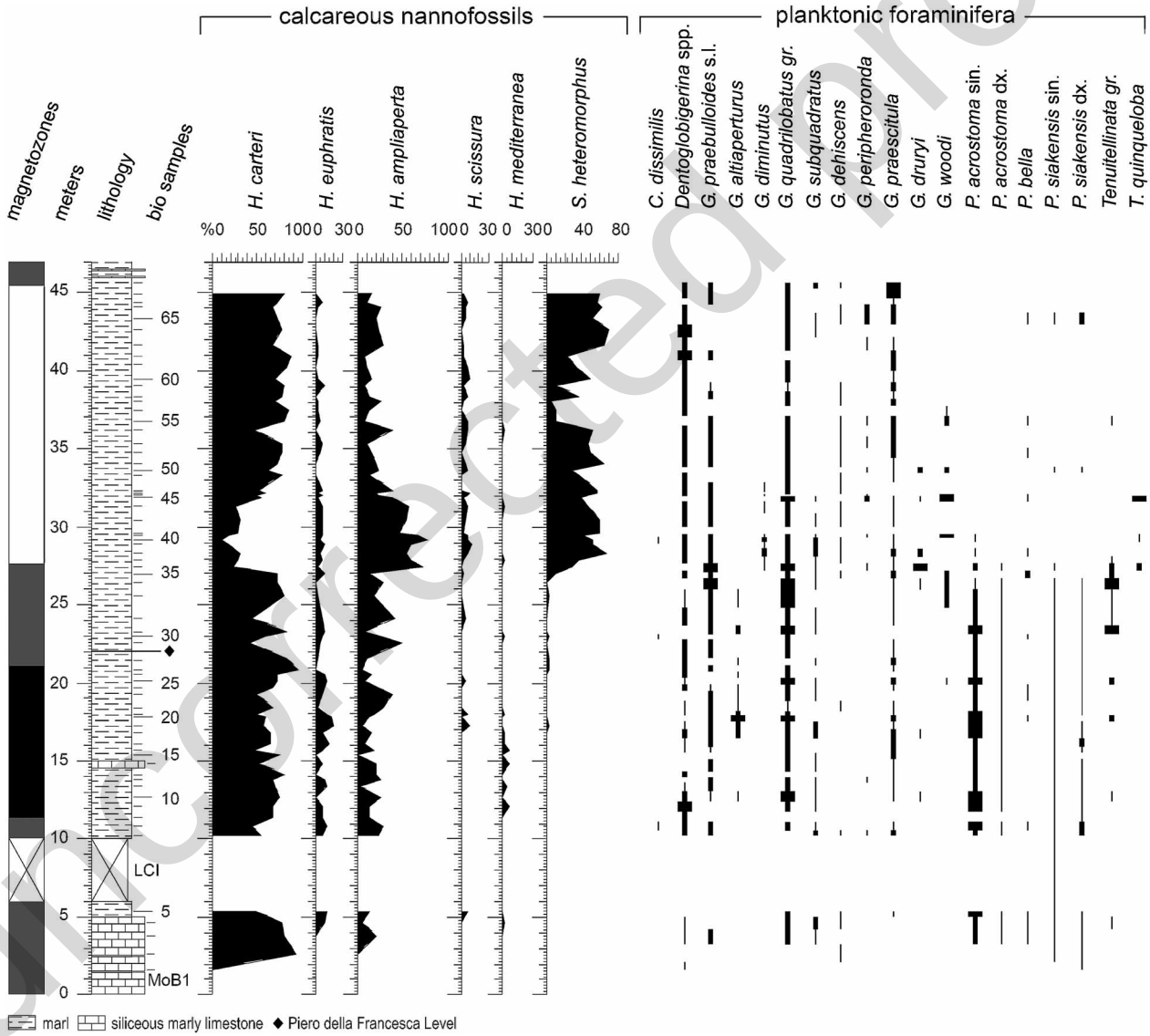

Fig. 6. Magnetostratigraphy and quantitative (calcareous nannofossil) and semi-quantitative (planktonic foraminifer) distribution patterns from the lower part of the Moria section. The black, white and gray areas indicate normal, reversal and uncertain polarity, respectively. LCI = Lower Covered Interval.

uncorrected proofs

Table 1 Magnetozones recognized in the Moria section.

POLARITY	THICKNESS (m)		INTERVAL Sample	INTERVAL Meters	MEAN (m)	ERROR +/- (m)	MAGNETO ZONE
Und. interval	1.70						
Reverse	1.10	T	MoP59	53.50	54.35	0.85	MR2
		B	MoP58	52.40	51.00	1.40	
Und. interval	2.80						
Normal	0.85	T	MoP56	49.60	51.00	1.40	MN2
		B	MoP56	49.60	47.50	2.10	
Und. interval	4.20						
Reverse	17.80	T	MoP53	45.40	47.50	2.10	MR1
		B	MoP31	27.60	24.40	3.20	
Und. interval	6.40						
Normal	9.80	T	MoP25	21.20	24.40	3.20	MN1
		B	MoP11	11.40	5.90	5.50	
Und. interval	11.00						

Catapsydrax dissimilis

The Last Occurrence (LO) of the genus *Catapsydrax* is considered a first-order bioevent and has been widely used for tropical open-ocean settings (Blow 1969, Berggren et al. 1995) and the Mediterranean region (Iaccarino 1985). The LO of *C. dissimilis* s.l. (Blow 1969, Kennett and Srinivasan 1983), or of *C. dissimilis/unicavus* according to Berggren et al. (1995), marks the top of the *Globigerinatella insueta/Catapsydrax dissimilis* zone (N6 and M3 biozones of Blow 1969 and Berggren et al. 1995, respectively).

In the examined samples, *Catapsydrax* is rare, and the poor preservation makes its distinction from *Globigerina venezuelana* and dentoglobigerinids sometimes difficult. The latter two taxa tend to form an aberrant small last chamber partially covering the umbilicus (Bolli and Saunders 1985), developing an element similar to the bulla in the genus *Catapsydrax*. *Catapsydrax dissimilis* is present up to sample MoB39 (29.0 m), close to the abundance increase of *Sphenolitus heteromorphus* (Fig. 6).

Globigerinoides altiaperturus

Globigerinoides altiaperturus has been used as a zonal marker in the lower Miocene of the Mediterranean region (Iaccarino 1985, Mancin et al. 2003, Iaccarino et al. 2007). Specimens with the typical high-arc apertures are present continuously in the middle part of the investigated section (samples MoB18–MoB31, 17.6–23.8 m). The absence of the taxon in the lower part is probably due to poor preservation. The highest presence of *G. altiaperturus* in sample MoB33 (Fig. 6) may represent the true LO of the species, in agreement with Iaccarino (1985) who reports a late Burdigalian age for this event.

Globigerinoides diminutus

Globigerinoides diminutus is morphologically similar to *G. ruber* and *G. subquadratus*, but has a smaller and more compact test as well as a higher and narrower aperture (Bolli and Saunders 1985). The species appears in the late Burdigalian N7 zone (Blow 1969, Postuma 1971, Salvatorini and Cita 1979, Kennett and Srinivasan 1983, Bolli and Saunders 1985, Iaccarino 1985).

According to Foresi et al. (2014), this species appears in the upper part of their *P. acrostoma/C. dissimilis* (MMi2c) subzone, which corresponds to Blow's (1969) N6 zone. The first occurrence (FO) of typical specimens is in sample MoB36 (28.0 m), just below the last common occurrence (LCO) of *P. acrostoma* and the LO of *C. dissimilis* (Fig. 6).

Globigerinoides quadrilobatus group

The group comprises *Globigerinoides quadrilobatus*, *G. sacculifer* and *G. trilobus*, which Blow (1969) considered to be subspecies of *G. quadrilobatus*. Specimens of this group are common and continuously present throughout the investigated section (Fig. 6), with *G. trilobus* and *G. quadrilobatus* being dominant.

Typical *G. trilobus* are accompanied by small and medium-sized specimens with ovoidal, sub-spherical or bi-spherical outline of the test, showing some affinity with the *Globigerinoides-Praeorbulina* group (Turco et al. 2011b). There are consistently two apertures at the base of the last chamber, and the wall texture is cancellate. Unfortunately, the poor preservation often hampers the identification of the secondary apertures. No convincing specimens with three apertures at the base of the last chamber were found; this implies that *G. sicanus* is absent from the investigated samples, which is consistent with the FO of the species located at a stratigraphically higher level in the Moria section (Di Stefano et al. 2008).

Globigerinoides subquadratus

Globigerinoides subquadratus is an important biostratigraphic marker for the Miocene. The FO of the taxon has been reported in the middle early Miocene (Blow 1969, Bizon and Bizon 1972, Kennett and Srinivasan 1983, Bolli and Saunders 1985, Iaccarino 1985, Spezzaferri 1994, Coccioni et al. 1997, Hakyemez and Toker 2010, Foresi et al. 2014). Typical specimens of *G. subquadratus*, with two supplementary apertures, occur from sample MoB3 (3.80 m) upsection, but this observation may be biased by diagenetic effects due to the poor preservation in the lower part of

Uncorrected proofs

the section (Fig. 6). The species shows a discontinuous distribution up to sample MoB41 (29.5 m), becoming further scattered upwards. The *G. subquadratus* concept includes very small specimens as they are mainly present in the basal part of the section; these specimens resemble *Globigerinoides diminutus*, from which they differ by the large secondary apertures, the incised intercameral sutures and the less box-shaped form of the test.

Globorotalia peripheroronda

The FO and LO of *G. peripheroronda* have been reported at the base of the Aquitanian (Kennett and Srinivasan 1983, Spezzaferri 1994) and in the Serravallian (Foresi et al. 2002, Hilgen et al. 2009), respectively. In the Mediterranean region, *G. peripheroronda* occurs from the late Burdigalian *Globigerinoides trilobus* zone onwards (Iaccarino 1985), but it is generally rare in the lower part of its range (Foresi et al. 2001, Lirer and Iaccarino 2005, Di Stefano et al. 2011b).

In the investigated samples, *G. peripheroronda* shows rare occurrences in two samples from the lower part of the succession, and rare to few discontinuous occurrences from sample MoB36 (27.4 m) upwards, together with *Turborotalita quinqueloba* (Fig. 6). This distribution pattern of the two taxa agrees with data from the St. Thomas section (Foresi et al. 2014), which crops out along the southeastern coast of Malta Island (Fig. 1).

Globorotalia praescitula

According to Iaccarino (1985), *G. praescitula* first occurs in the Burdigalian *G. trilobus* zone and becomes common in the Mediterranean region during the Langhian (Foresi et al. 2001). In the Moria section, the first specimens of *G. praescitula* were found in sample MoB5 (5.40 m). The species is rare to common and has a discontinuous occurrence upwards, which confirms the scattered distribution reported by Deino et al. (1997). Considering the poor preservation of foraminifers in the lower part of the section, it cannot be excluded that this species also occurs below sample MoB5.

Paragloborotalia acrostoma

The stratigraphic distribution of *P. acrostoma* is reported from the latest Oligocene to early Langhian by Spezzaferri (1994, 1996), but according to Foresi et al. (2001) the species is typical of the early-early middle Miocene. In the Moria section, the first specimens of *P. acrostoma* occur in sample MoB3 (3.80 m). The species shows a prevailing sinistral coiling and is common to abundant up to sample MoB36 (27.4 m). Its LCO is close to the LO of *C. dissimilis*. These two bioevents basically occur at the same level in other Mediterranean sections as well, such as at Colle Amarena (Lirer et al. 2007) and Pianosa (Cornamusini et al. 2014). In the uppermost part of its distribution range, *P. acrostoma* is rare. Its highest occurrence is in sample MoB41 (29.5 m).

Paragloborotalia siakensis

The stratigraphic distribution of *P. siakensis* ranges from the Oligocene to the Tortonian; it has been studied in detail as it is considered extremely useful for correlation of middle Miocene sections on the basis of alternating acme and paracme intervals (Dall'Antonia et al. 2001, Sprovieri et al. 2002, Di Stefano et al. 2008, 2011b). *Paragloborotalia siakensis* occurs rarely, but continuously from the base of the Moria section up to sample MoB36 (27.4 m), whereas it is scattered from this level upsection. The species shows random coiling patterns along its entire range in the Moria section.

Other taxa

Other members of the planktonic foraminiferal assemblages are of secondary biostratigraphic interest. They include the following taxa:

Dentoglobigerina spp. and *Globigerina praebulloides* s.l., are common to abundant and occur continuously throughout the Moria section. *Dentoglobigerina* spp. comprise predominantly *D. altispira* and subordinately *D. baroemoenensis*. According to Blow (1959, 1969) and Blow and Banner (1966), the early Miocene *G. praebulloides* comprises several morphotypes and subspecies. In the samples from the Moria section, this taxon is referred to as *G. praebulloides* s.l., which comprises *G. praebulloides praebulloides*, *G. praebulloides occlusa*, and *G.* aff. *falconensis*.

Paragloborotalia bella is present in the Moria Section, but occurs rarely and discontinuously. The *Tenuitellinata* group comprises typical specimens of *T. angustiumbilicata* and other five-chambered globigerinids. Some of these resemble *G. ciperoensis* due to a wide umbilical area, but have a smooth rather than cancellate text surface. The *Tenuitellinata* group is discontinuously present in the lower part of the Moria section, where it is abundant from samples MoB31 to MoB36 (23.2–27.4 m), and virtually absent in the uppermost part.

Globoturborotalita woodi and *G. druryi* only occur in the middle part of the Moria section. *Globoquadri-*

uncorrected proofs

na dehiscens is consistently rare and shows discontinuous occurrences throughout the section. Finally, *Turborotalita quinqueloba*, represented also by specimens showing the typical, slightly elongate last chamber covering the umbilicus, is present only in the interval from samples MoB35 to MoB45 (27.0–31.9 m). The comparison with the Foresi et al. (2014) St. Thomas section allows us to consider the lowest presence of the taxon in the Moria section as its stratigraphical FO.

6.2 Calcareous nannofossils

The calcareous nannofossil assemblages are characterized by poor preservation in the basal calcareous strata of the Bisciaro Fm (Fig. 6). Preservation is medium to good in the remainder of the section. The nannofossil associations consist of placoliths, helicoliths and sphenoliths; discoasterids are rare, occur sporadically and are almost exclusively represented by *Discoaster deflandrei*. Within the placoliths, estimated through a qualitative analyses, the most representative are *Coccolithus pelagicus*, *Cyclicargolithus floridanus*, *Dictyococcites* spp., and "small" and "medium" *Reticulofenestra*.

Following the most recent literature on Miocene nannofossil biostratigraphy in the Mediterranean region (Di Stefano et al. 2008, 2011b, Foresi et al. 2011, 2014, Iaccarino et al. 2011, Mourik et al. 2011, Turco et al. 2011a), helicoliths and sphenoliths were selected for quantitative analyses (Fig. 6) in order to determine positions of biostratigraphic horizons.

Helicosphaera carteri and *H. euphratis*

Among the helicoliths, *H. carteri* is the most common (average percentages $> 60\%$) taxon. It is continuously present in most of the analyzed samples, with the exception of the central part of the succession (28–32 m) where it is replaced by *H. ampliaperta*. *Helicosphaera euphratis* occurs in all samples, even if it only sporadically exceeds percentages of 10%. Fornaciari and Rio (1996) and more recently Backman et al. (2012) have highlighted the close inverse abundance relationship of *H. carteri* and *H. euphratis*. They used the sharp quantitative decrease of *H. euphratis* and the concomitant increase of *H. carteri* (reported as "*H. euphratis*/*H. carteri* cross-over") to define the boundary between the MNN1/MNN2a (Fornaciari and Rio 1996) and the CNM3/CNM4 (Backman et al. 2012) zones in the late Aquitanian. The high abundance of *H. carteri* together with the low abundance of *H. euphratis* suggests that the base of the section is younger than the *H. euphratis*/*H. carteri* cross-over dated at 20.9 Ma (Backman et al. 2012).

Helicosphaera ampliaperta and *H. scissura*

Helicosphaera ampliaperta is almost continuously present across the Moria section, becoming abundant between 28 and 30 meters (samples MoB36 to MoB44) where it accounts for more than 50% of the total helicoliths. The distribution of *H. ampliaperta* spans from the Aquitanian (Young 1998) to the middle Langhian (Di Stefano et al. 2008). In Lourens et al. (2004), its FO is adopted to provisionally approximate the Aquitanian/Burdigalian boundary at 20.43 Ma. The basal part of its range is discontinuous and characterized by temporary absence intervals (Gartner 1992, Fornaciari and Rio 1996, Foresi et al. 2014). The LCO of the species appears sharp and synchronous, while its LO seems to be diachronous among different sections in the Mediterranean region (Di Stefano 1995, Fornaciari et al. 1996, Di Stefano et al. 2008, 2011b, Foresi et al. 2011, Iaccarino et al. 2011, Turco et al. 2011a).

Data from the Central Paratethys suggest that *H. ampliaperta* may have evolved from *H. scissura*, whose FO is recorded in the early Aquitanian (Marunteanu 1999, Rögl and Nagymarosy 2004, Garecka 2005, Bartol 2009, Makrodimitras et al. 2010, Chira et al. 2011, Holkova 2013). For open-ocean settings, the FO of *H. scissura* is reported in the middle Burdigalian, at about 18.28 Ma, thus following that of *H. ampliaperta* (Young 1998). In Mediterranean sequences the two species generally occur together, and it is difficult to establish which one represents the ancestor of the other.

In the Moria samples, *H. scissura* exhibits low abundances ($< 10\%$) and a discontinuous distribution, but seems to match the distribution pattern of *H. ampliaperta*. *Helicosphaera scissura* may hence represent a morphotype within the *H. ampliaperta* population.

Helicosphaera mediterranea

Helicosphaera mediterranea is a lower–middle Miocene species, spanning from the early Aquitanian to the late Langhian (Theodoridis 1984). Marunteanu (1999) recognizes a basal Miocene age (NN1 zone of Martini 1971) for the FO of this taxon in the Carpathian region, in contrast to the early Burdigalian age (MNN2a zone) proposed by Fornaciari and Rio (1996) for the Mediterranean region. Furthermore, in some Mediterranean sections, the FO of *H. mediterranea* precedes that of *H. ampliaperta*, whereas in others this event seems to be younger (Fornaciar and Rio 1996). Thus, the relation between *H. mediterranea* and *H. ampliaperta* is still

Uncorrected Proofs

controversial. However, the Moria section, where the taxon shows a low and discontinuous occurrence from the basal levels onwards, is not suitable to solve this conundrum.

Sphenolithus heteromorphus

Sphenolithus heteromorphus is absent or rare in the lower part of the investigated succession. Sporadic specimens are recorded in a few samples from about 18 to 28 meters (Fig. 6). From this level upwards, the species becomes continuously present, with average percentages of about 30% and a maximum of about 70% with regard to the total sphenolith assemblages.

The FO of *S. heteromorphus* has been used by Okada and Bukry (1980) to define the base of their CN3 zone and by Theodoridis (1984) to recognize the boundary between its *Sphenolithus belemnos* subzone and *Helicosphaera ampliaperta* zone. Moreover, Fornaciari and Rio (1996) and Backman et al. (2012) used the FCO of the taxon to define the base of their MNN3b and CNM6 zones, respectively. In its initial range *S. heteromorphus* is generally accompanied by discontinuous, low-percentage occurrences of *S. belemnos*, whose LCO is below the FO of *S. heteromorphus* (Fornaciari and Rio 1996, Raffi et al. 2006). In the Moria section, *S. belemnos* is absent, which may suggest that the first specimens of *S. heteromorphus* recorded at the base of the section do not represent its true biostratigraphical FO.

7. Magnetostratigraphic interpretation and age model

The age-model herein proposed refers to the entire Moria Section (sensu Deino et al. 1997; composite Moria Section in Figs. 1, 7, and 8) and has been obtained through the integration of the data from the present study and those of Di Stefano et al. (2008). The two portions of the section were correlated using the calcareous marker horizons in the middle member of the Schlier Fm (Figs. 2, 3). This allows to define biostratigraphic events for the entire succession and to extend the age-model upsection where paleomagnetic data are absent. The data from the entire Moria section have been compared to data from other Mediterranean sections and from North Atlantic DSDP Site 608 (Figs. 1, 8; Tables 2, 3).

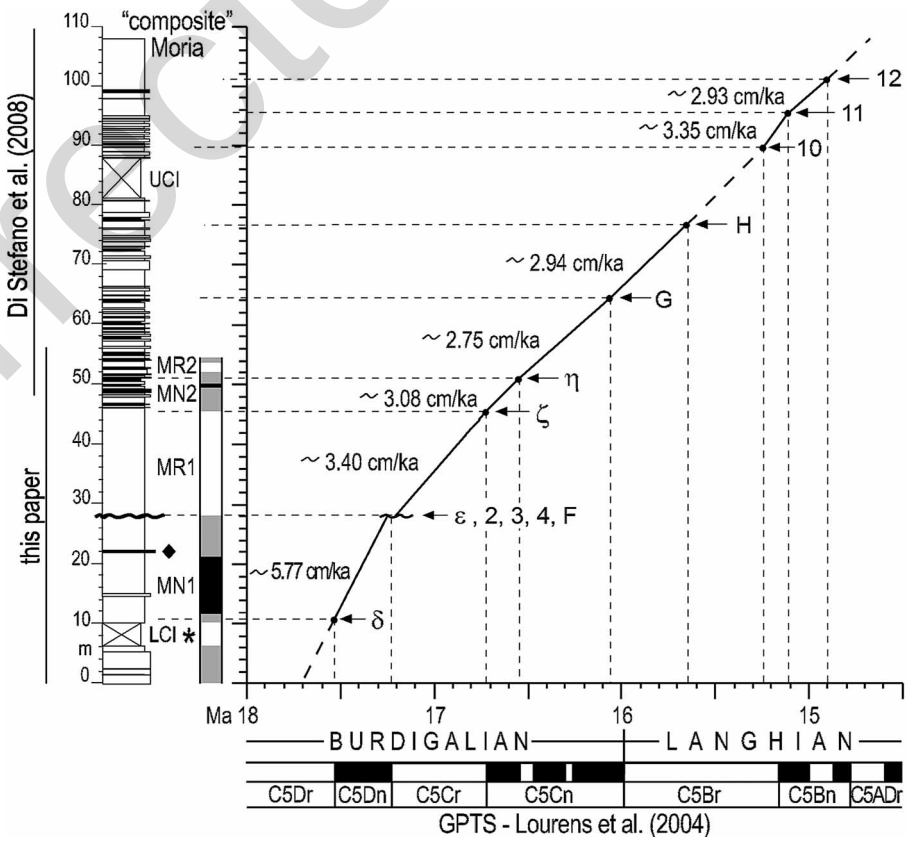

Fig. 7. Age-depth diagram and estimated sedimentation rates for the composite Moria section. Numbers and greek letters associated with arrows refer to the bio- and magnetostratigraphic events listed in Table 3; (*) in Deino et al. 1997. The part considered in the present study and the part examined by Di Stefano et al. (2008) are indicated. LCI = Lower Covered Interval; UCI = Upper Covered Interval.

Uncorrected proofs

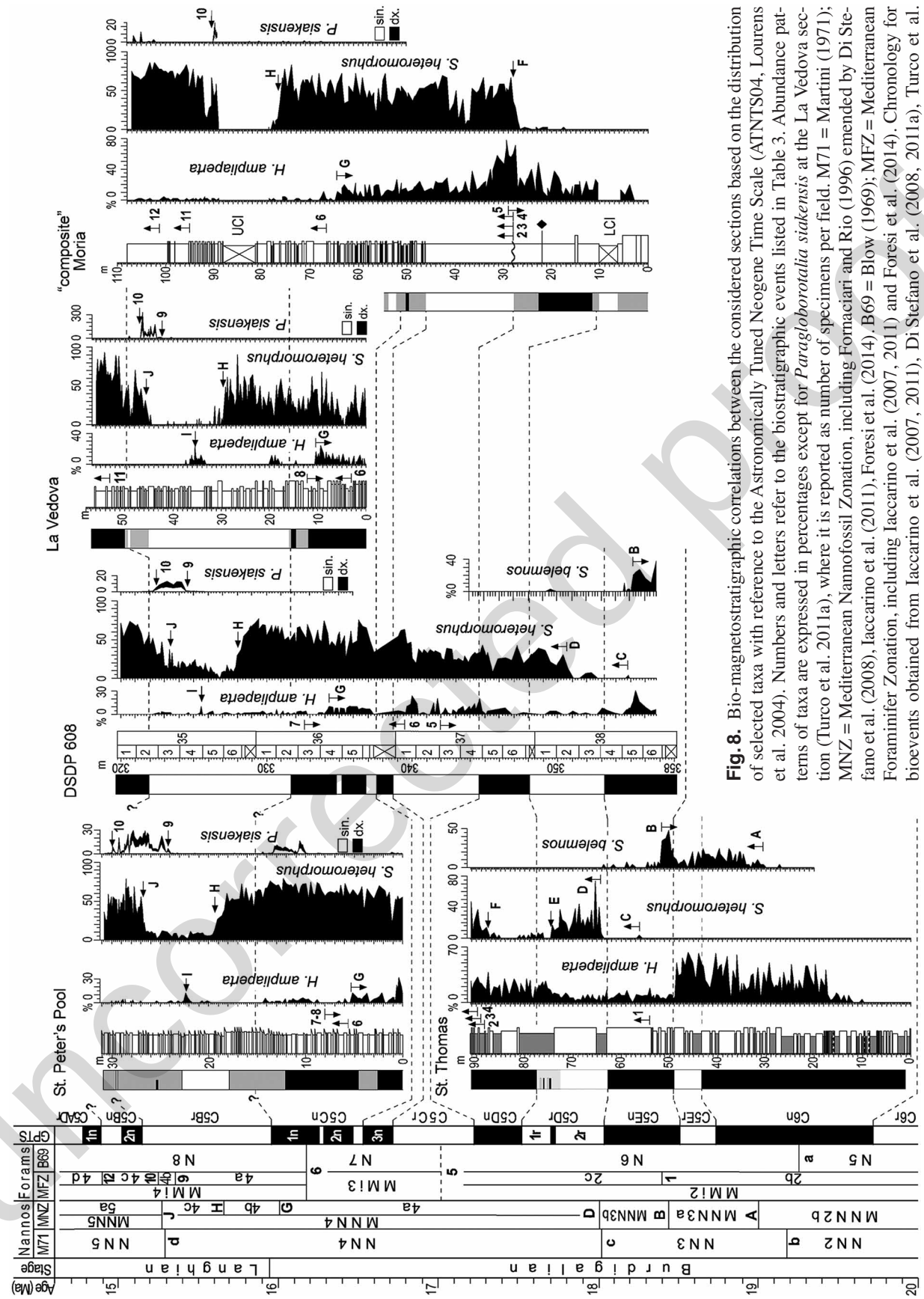

Fig. 8. Bio-magnetostratigraphic correlations between the considered sections based on the distribution of selected taxa with reference to the Astronomically Tuned Neogene Time Scale (ATNTS04, Lourens et al. 2004). Numbers and letters refer to the biostratigraphic events listed in Table 3. Abundance patterns of taxa are expressed in percentages except for *Paragloborotalia siakensis* at the La Vedova section (Turco et al. 2011a), where it is reported as number of specimens per field. M71 = Martini (1971); MNZ = Mediterranean Nannofossil Zonation, including Fornaciari and Rio (1996) emended by Di Stefano et al. (2008), Iaccarino et al. (2011), Foresi et al. (2014). B69 = Blow (1969); MFZ = Mediterranean Foraminifer Zonation, including Iaccarino et al. (2007, 2011) and Foresi et al. (2014). Chronology for bioevents obtained from Iaccarino et al. (2007, 2011), Di Stefano et al. (2008, 2011a), Turco et al. (2011b), and Foresi et al. (2014). LCI = Lower Covered Interval; UCI = Upper Covered Interval.

Uncorrected Proofs

The base of the Moria section (this study) is characterized by poorly preserved calcareous plankton assemblages and a lack of reliable paleomagnetic data, while the interval from 11 to 21 m shows a clear normal polarity (magnetozone MN1). The first specimens of *S. heteromorphus* fall within this interval. Comparison with data from St. Thomas and DSDP Site 608 suggests that this is not the FO of the species as indicated by the absence of *S. belemnos* in the Moria section. Rather, the discontinuous and low abundance interval of *S. heteromorphus* appears coeval with the "paracme P_0" in the St. Thomas section of Foresi et al. (2014). These authors report the base of *S. heteromorphus* P_0 at the C5Dr/C5Dn boundary. This suggests that the normal interval MN1 can be interpreted as

Table 2 Summary of the sections considered in this paper and main references.

SECTION / CORE	LOCATION	COORDINATES	REFERENCES
St. Thomas	SE Malta Island	35°50.44'N; 14°34.01'E	Foresi et al. (2014)
St. Peter's Pool	SE Malta Island	35°49.98'N; 14°33.71'E	Foresi et al. (2011), Iaccarino et al. (2011)
La Vedova	Marche Region (Italy)	43°35.41'N; 13°33.81'E	Montanari et al. (1995, 1997), Mader et al. (2001, 2004), Husing et al. (2010), Iaccarino et al. (2011), Turco et al. (2011a)
"composite" Moria	Marche Region (Italy)	43°30.14'N; 12°35.48'E	Fornaciari and Rio (1996), Fornaciari et al. (1996), Deino et al. (1997), Di Stefano et al. (2008)
DSDP Hole 608	NE Atlantic Ocean	42°50.205'N; 23°05.252'W	Baldauf et al. (1987), Ruddiman et al. (1987), Miller et al. (1991), Olafsson (1991), Gartner (1992), Krijgsman and Kent (2004), Di Stefano et al. (2011a)

Table 3 Magnetostratigraphic calibration (ATNTS2004, Lourens et al. 2004) and ages (where available) of the main biohorizons recognized within the "composite" Moria section (Di Stefano et al. 2008 and this paper), La Vedova (Iaccarino et al. 2011, Turco et al. 2011a), St. Thomas (Foresi et al. 2014), St. Peter's Pool (Foresi et al. 2011, Iaccarino et al. 2011), and DSDP Site 608 (Di Stefano et al. 2011a, this paper). Acronyms for the biohorizons: FO = First Occurrence; FCO = First Common Occurrence; LO = Last Occurrence; LCO = Last Common Occurrence; AB-r/s = Acme Base and coiling change from random to sinistral; P_0B = Paracme$_0$ Base; P_0E = Paracme$_0$ End; AS = Abundance Spike; AaB = Acme a Base; AaE = Acme a End.

BIOEVENTS and MAGNETOCHRONS			"COMPOSITE" MORIA			LA VEDOVA			ST. THOMAS			ST PETER'S POOL		DSDP 608		
			sample	meters	Chron/Age (Ma)	meters	Chron	Age (Ma)	meters	Chron	Age (Ma)	meters	Chron	mbsf	Chron	Age (Ma)
12	FO	*P. glomerosa circularis*	MOR303	101.34												
11	FO	*P. glomerosa glomerosa*	MOR266	95.01		53.01	C5Bn.2n	15.106								
ι		C5Br-C5Bn						15.160						322.36		15.160
10	AaE	*P. siakensis*	MOR225	89.9		46.17	C5Br/C5Bn.2n	15.246				29.91	C5Br	321.95	C5Br/C5Bn.2n	15.138
d	LO	*H. ampliaperta*												322.33	C5Br	15.167
J	PE	*S. heteromorphus*				45.54	C5Br/C5Bn.2n	15.261				26.83	C5Br	322.95	C5Br	15.254
9	AaB	*P. siakensis*				41.35	C5Br	15.361				24.19	C5Br	324.05	C5Br	15.322
I	AS	*H. ampliaperta*				35.40	C5Br					22.33	C5Br	325.55	C5Br	15.475
H	PB	*S. heteromorphus*	MOR198	76.62		29.58	C5Br	15.644				19.37	C5Br	327.95	C5Br	15.656
θ		C5Cn-C5Br				15.90		15.974						332.23		15.974
8	LCO	*P. bella*				12.11	C5Cn.1n	16.030				7.82	C5Cn.1n			
7	LCO	*G. peripheroronda*										7.82	C5Cn.1n	332.57	C5Cn.1n	16.054
6	FO	*G. sicanus=P. glom. sic.*	MOR120	66.70		3.08	C5Cn.1n	16.177				5.68	C5Cn.1n	339.45	C5Cr	16.844
G	LCO	*H. ampliaperta*	MOR108	64.41		10.38	C5Cn.1n	16.057				5.12	C5Cn.1n	334.15	C5Cn.1n	16.160
η		C5Cn.3n/C5Cn.2r			16.543									337.60		16.543
ζ		C5Cr-C5Cn			16.721									338.75		16.721
5	LO	*C. dissimilis*	MoB39	29.00	C5Cr									341.94	C5Cr	17.003
ε		C5Dn/C5Cr			17.235									344.69		17.235
4	FO	*G.peripheroronda*	MoB36	27.40	C5Dn/C5Cr				89.79	C5Dn	17.277					
3	FO	*T. quinqueloba*	MoB36	27.40	C5Dn/C5Cr				89.17	C5Dn	17.288					
2	FO	*G. diminutus*	MoB36	27.40	C5Dn/C5Cr				88.40	C5Dn	17.293					
F	P_0E	*S. heteromorphus*	MoB36	27.40	C5Dn/C5Cr				87.60	C5Dn	17.311					
δ		C5Dr/C5Dn			17.533						17.533			348.50		17.533
E	P_0B	*S. heteromorphus*							74.66	C5Dr/C5Dn	17.558					
D	FCO	*S. heteromorphus*							64.58	C5Dr	17.992			350.80	C5Dr	
c	LO	*S. belemnos*							63.72	C5Dr	18.022					
γ		C5En/C5Dr							62.93		18.056			353.28		18.056
C	FO	*S. heteromorphus*							56.30	C5En	18.290			354.85	C5En	
1	AB-r/s	*P. acrostoma*							53.17	C5En	18.400					
B	LCO	*S. belemnos*							51.45	C5En	18.436			355.23	C5En	
β		C5Er/C5En							49.10		18.524					
α		C6n/C5Er							43.26		18.748					
A	FCO	*S. belemnos*							30.59	C6n	19.047					
b	LO	*T. carinatus*														
a	FO	*G. insueta*														

uncorrected proofs

Chron C5Dn (17.533–17.235 Ma, Lourens et al. 2004) (Figs. 7, 8).

In the Moria section (this study), the FOs of *Globigerinoides diminutus*, *Turborotalita quinqueloba* and *Globorotalia peripheroronda*, and the end of the lower paracme of *Spenolithus heteromorphus* (P_0E) (see events 2, 3, 4 and F, respectively, in Table 3) occur at the same stratigraphic level (28 m), close to the base of the MR1 magnetozone. In the St. Thomas section, events 2, 3 and 4 occur at different stratigraphic levels in upper Chron C5Dn. There, the *S. heteromorphus* P_0E also occurs within Chron C5Dn, slightly preceding the abovementioned foraminiferal events. This comparison allows to draw the following conclusions regarding the Moria section: i) the interval characterized by absence of paleomagnetic signals from 23 to 28 m has been deposited during Chron C5Dn time; ii) MR1 can be referred to Chron C5Cr; iii) a short hiatus involving the C5Dn/C5Cr boundary is present at about 28 m; this can be estimated to have lasted at least 34 ka, which represents the difference of the ages between the *S. heteromorphus* P_0E and the FO of *G. peripheroronda* as determined by Foresi et al. (2014), as 17.311 Ma and 17.277 Ma, respectively. Consequently, MN2 has been interpreted as Chron C5Cn.3n, MR2 as Chron C5Cn.2r, and the reverse magnetozone recognized by Deino et al. (1997) at the base of the section (Fig. 2) as Chron C5Dr.

For the Moria section, the age model presented in Fig. 7 takes into account the bio-magnetostratigraphic data of the present study and the position of the bioevents determined by Di Stefano et al. (2008), with ages derived from the neighbour La Vedova section (Table 3, Iaccarino et al. 2011, Turco et al. 2011a) and, for the lower portion, from the Maltese St. Thomas section (Table 3, Foresi et al. 2014). From 28 m upwards, the distribution of the bio-magnetostratigraphic events suggests near-constant sedimentation rates, with an average of about 3 cm/ka. In the lower part, the sedimentation rate slightly exceeds 5 cm/ka, in spite of the presence of a short hiatus. The average sedimentation rate, calculated from the top of the lower vegetation-covered interval (10 meters above the base of the section and marked as LCI in Figs. 3, 7) to the top of the composite section (ca. 108 meters from the base; Fig. 7) is 3.85 cm/ka, which is in close agreement with the sedimentation rate of ca. 4.0 cm/ka reported by Capuano (2009) for the Schlier Fm in the Urbino area (northern sector of the Marche region).

The proposed age model for the composite Moria section suggests deposition between about 17.7 and 14.7 Ma, corresponding to a late Burdigalian–Langhian age (Lourens et al. 2004); this is in agreement with the radiometric age of the "Piero della Francesca Level" reported by Deino et al. (1997). From a biostratigraphic perspective, the Moria section represents the interval between nannofossil biozones MNN4a and MNN5a, and between planktonic foraminifer biozones MMi2c and MMi4d (Di Stefano et al. 2008, Iaccarino et al. 2011, Foresi et al. 2014).

8. Mediterranean-Atlantic correlation

The lower part of the Moria section (sensu Deino et al. 1997) here investigated in detail is instrumental for generating a bio-magnetostratigraphy of the early to middle Miocene interval of the Mediterranean region. To achieve this goal, the composite Moria section has been correlated with other Mediterranean successions (Figs. 1, 8; Tables 2, 3). A series of magnetostratigraphically constrained calcareous plankton bioevents has been established that covers the time interval from about 19.7 Ma (base of the St. Thomas section) to about 14.7 Ma (top of the composite Moria section). Furthermore, the comparison of the results of Mediterranean sections to a reference succession in the Atlantic Ocean (DSDP Site 608) (Miller et al. 1991, Olafsson 1991, Gartner 1992, Krijgsman and Kent 2004, Di Stefano et al. 2011a, Wade et al. 2011) allowed us to discriminate between the events with a both Mediterranean and extra-Mediterranean biostratigraphical significance and those with more regional importance.

Besides the well-known, yet debated bioevents (such as the LCO and LO of *H. ampliaperta*) horizons based on abundance fluctuations of selected species merit special attention. These biohorizons, although seemingly less trustworthy than proper FOs and LOs, provide useful and reliable biostratigraphic constraints for the considered time interval. The best-known example is probably the *Sphenolithus heteromorphus* "Paracme Interval" (Di Stefano 1995, Fornaciari et al. 1996) (H and J in Fig. 7 and Table 3), which is recorded almost synchronously in numerous Mediterranean sections (Iaccarino et al. 2011) and at Site DSDP 608 (Di Stefano et al. 2011a). In the same way, the *Paragloborotalia siakensis* "Acme a Interval" (Dall'Antonia et al. 2001, Di Stefano et al. 2008) (events 9 and 10 in Fig. 8 and Table 3) is a sharp interval clearly detectable both in the Mediterranean and North Atlantic

Uncorrected Proofs

successions. Conversely, the older *S. heteromorphus* paracme ("Paracme 0" in Foresi et al. 2014) detected in the Mediterranean region at the top of the St. Thomas section (events E and F in Fig. 8 and Table 3) and at the base of the Moria Section, but missing in the Atlantic DSDP 608 succession, may be only of regional value as correlation tool. Similarly, other abundance peaks, such as the one of *P. siakensis* recognized in the intermediate part of the St. Peter's Pool section ("Acme$_0$" in Foresi et al. 2011, absent in the same levels of the La Vedova section of Turco et al. 2011), which crops out along the southeastern coast of Malta Island (Fig. 1) can also be considered of regional value and are possibly related to regional environmental conditions (Iaccarino et al. 2011).

The comparison between the St. Thomas section and the basal part of DSDP Site 608 clarifies the relationship between the final distribution range of *S. belemnos* (above its LCO) and the FO of *S. heteromorphus* in the frame of tight magnetostratigraphic control. The LCO of *S. belemnos* represents a well-defined event and is recorded within Chron C5En both in the St. Thomas section and at DSDP Site 608, while the LO of the species occurs at higher stratigraphic levels within Chron C5Dr. The stratigraphic positions of the FO and FCO of *S. heteromorphus* have been repeatedly debated in the literature (Martini 1971, Okada and Bukry 1980, Olafsson 1991, Gartner 1992, Fornaciari and Rio 1996, Backman et al. 2012). At DSDP Site 608, the FO of *S. heteromorphus* occurs between the LCO and the LO of *S. belemnos*, within Chron C5En. This is in good agreement with the St. Thomas section, where the FO of *S. heteromorphus* occurs in the same chron, within the final distribution range of *S. belemnos*. The FCO of *S. heteromorphus* occurs within Chron C5Dr in both the sections.

The LO of *C. dissimilis* is another discussed bioevent, reported to be within Chron C5Dn by Berggren et al. (1983), at 17.5 Ma by Shackleton et al. (1999) (C5Dr/C5Dn transition in Figs. 2 and 3 of Wade et al. 2011), and within Chron C5Cr by Di Stefano et al. (2011a). The occurrence of the last *C. dissimilis* specimens at the base of Chron C5Cr in the Moria section agrees with its position at DSDP Site 608 (Di Stefano et al. 2011a). Yet, this event does not seem to represent a reliable correlation tool within the Mediterranean area because in some cases, for example the St. Thomas section, the species is completely absent, probably due to environmental factors (Foresi et al. 2014).

9. Conclusions

Results are presented from an integrated bio-magnetostratigraphic study of the lower segment of the Moria section (sensu Deino et al. 1997), cropping out in the Umbria–Marche Apennine (Central Italy). According to our reconstruction, this portion of the section ranges from the top of Chron C5Dr to Chron C5Cn.2r, almost continuously spanning from about 17.7 to 16.4 Ma (according to the ATNTS04), with a small hiatus, estimated in at least 34 ka, at the C5Dn/C5Cr transition. This interpretation differs from that of Deino et al. (1997), but is consistent with the radiometric age of 17.1 ± 0.16 Ma reported by the same authors for the "Piero della Francesca Level" in the section.

An age model is proposed for the composite Moria Section, based on the bio-magnetostratigraphic data of the present study and the biostratigraphic results of Di Stefano et al. (2008). It is chronologically constrained through a comparison with the La Vedova section (Turco et al. 2011). According to our reconstruction, the composite Moria section covers about 3 Ma (17.7–14.7 Ma), thus straddling the Burdigalian/Langhian boundary (Lourens et al. 2004, Iaccarino et al. 2011).

Calcareous plankton data from the composite Moria section are compared with previously published datasets from other Mediterranean sections. This yields a magnetostratigraphically framed calcareous plankton dataset that covers a time interval of about 5 Ma from the base of the St. Thomas section at 19.7 Ma to the top of the composite Moria Section at 14.7 Ma.

The presence/absence of biostratigraphical events as deduced from a comparison of datasets from the Mediterranean region and North Atlantic DSDP Site 608 enabled us to discriminate between bioevents exportable in extra-Mediterranean areas from those showing a bioprovincial or local stratigraphic significance.

Acknowledgements. Fabrizio Lirer and Federica Zangara are thanked for their help during the sampling. We are indebted to three anonymous reviewers for their constructive suggestions. The study has been conducted within the project "PRIN2012" entitled "The Burdigalian GSSP (Global Stratigraphic Section and Point): the missing tile to complete the Neogene interval of the Geological Time scale", financed by the Italian MIUR and coordinated by Agata Di Stefano.

Uncorrected Proofs

References

Backman, J., Raffi, I., Rio, D., Fornaciari, E., Pälike, H., 2012. Biozonation and biochronology of Miocene through Pleistocene calcareous nannofossils from low and middle latitudes. Newsletters on Stratigraphy **45**(3), 221–244.

Baldauf, J.G., Thomas, E., Clement, B., Takayama, T., Weaver, P.P.E., Backman, J., Jenkins, G., Mudie, P.J., Westberg-Smith, M.J., 1987. Magnetostratigraphic and biostratigraphic synthesis, Deep Sea Drilling Project Leg 94. In: Ruddiman, W.F., Kidd, R.B., Baldauf, J.G. (Eds.), Initial Reports, Deep Sea Drilling Project 94. Washington, D.C., Government Printing Office, p. 1159–1205.

Bartol, M., 2009. Middle Miocene calcareous nannoplankton of NE Slovenia (Western Central Paratethys). Ph.D. Thesis, Paleontološki inštitut Ivana Rakovca ZRC SAZU, Ljubljana, Slovenia, 142 p.

Berggren, W.A., Hamilton, N., Johnson, D.A., Pujol, C., Weiss, W., Čepek, P., Gombos, A.M., 1983. Magnetostratigraphy of Deep Sea Drilling Project Leg 72, Sites 515–518, Rio Grande Rise (South Atlantic). In: Barker, P.F., Johnson, D.J., Carlson, R.J., et al. (Eds.), Initial Reports DSDP 72. Washington, United States, p. 675–714.

Berggren, W.A., Kent, D.V., Swisher III, C.C., Aubry, M.-P., 1995. A revised Cenozoic geochronology and chronostratigraphy. In: Berggren, W.A., Kent, D.V., Aubry, M.-P., Hardenbol, J. (Eds.), Geochronology, Time Scales and Global Stratigraphic Correlation: A unified temporal framework for an historical geology. Society of Economic Paleontologists and Mineralogists (SEPM) Special publication **54**, p. 129–212.

Bizon, G., Bizon, J.J., 1972. Atlas des principaux foraminifères planctoniques du Bassin Méditerranéen. Oligocene à Quaternaire. Ed. Technip, Paris, 316 p.

Blow, W.H., 1959. Age, correlation and biostratigraphy of the upper Tocuyo (San Lorenzo) and Pozon Formations, eastern Falcon, Venezuela. Bulletin of American Paleontology **39**(178), 67–252.

Blow, W.H., 1969. Late Middle Eocene to Recent planktonic Foraminifera biostratigraphy. Proceedings of the 1th International Conference on Planktonic Microfossils. Geneva, Switzerland, 1967, p. 199–421.

Blow, W.H., Banner, F.T., 1966. The morphology, taxonomy and biostratigraphy of *Globorotalia barisanensis* LeRoy, *Globorotalia fohsi* Cushman and Ellis, and related taxa. Micropaleontology **12**(3), 286–302.

Bolli, H.M., Saunders, J.B., 1985. Oligocene to Holocene low latitude planktic foraminifera. In: Bolli, H.M., Saunders, J.B., Perch-Nielsen, K. (Eds.), Plankton Stratigraphy. Cambridge University Press, New York, p. 155–262.

Capuano, N., 2009. Note illustrative della carta geologica d'Italia alla scala 1:50.000, Foglio 279 URBINO. Ispra, Roma, 114 p.

Chadima, M., Hrouda, F., 2006. Remasoft 3.0a user-friendly paleomagnetic data browser and analyzer. Travaux Géophysiques, **27**, 20–21.

Chira, C.M., Igritan, A., Juravle, D.T., Florea, F., Popa, V., 2011. Calcareous nannoplankton across the Paleogene–Neogene boundary in the Moldovita-Paltinu area (Bucovina, Romania). Acta Palaeontologica Romaniae **7**, 93–101.

Coccioni, R., Montanari, A., 1992. The "Livello Piero della Francesca" in the Umbria–Marche Apennines, Italy: a regional volcaniclastic marker bed at the boundary between the Bisciaro and the Schlier/Marne con Cerrogna formations (Lower Miocene). In: Montanari, A., Coccioni, R., Odin, G.S. (Eds.), Volume of Abstracts and Field Trips, Interdisciplinary Geological Conference on the Miocene Epoch with emphasis on the Umbria–Marche sequence (I.U.G.S., Subcommission on Geochronology, Miocene Columbus Projects). Ancona, Italy, p. 41–42.

Coccioni, R., Montanari, A., 1994. L'orizzonte del Bisciaro. In: Guide Geologiche Regionali, Appennino umbro-marchigiano, 7, BE-MA Editrice, p. 36–38.

Coccioni, R., Montanari, A., Fornaciari, E., Rio, D., Zevenboom, D., 1997. Potential integrated stratigraphy of the Aquitanian to upper Burdigalian section at Santa Croce di Arcevia (NE Apennines, Italy). In: Montanari, A., Odin, G.S., Coccioni, R. (Eds.), Miocene Stratigraphy: an integrated approach. Elsevier Science B.V., Amsterdam, p. 279–295.

Cornamusini, G., Foresi, L.M., Dall'Antonia, B., Bossio, A., Mazzei, R., Salvatorini, G., 2014. The Miocene of the Pianosa Island: a key for the puzzle on the opening of the Northern Tyrrhenian back-arc basin (Central Mediterranean). Journal of the Geological Society **171**, 801–819.

Dall'Antonia, B., Di Stefano, A., Foresi, L.M., 2001. Integrated micropalaeontological study (ostracods and calcareous plankton) of the Langhian western Hyblean succession. Palaeogeography, Palaeocology, Palaeoeclimatology **176**, 59–80.

Deino, A., Channell, J., Coccioni, R., De Grandis, G., De Paolo, D.J., Fornaciari, E., Emmanuel, L., Laurenzi, M.A., Montanari, A., Rio, D., Renard, M., 1997. Integrated stratigraphy of the upper Burdigalian–lower Langhian section at Moria (Marche Region, Italy). In: Montanari, A., Odin, G.S., Coccioni, R. (Eds.), Miocene Stratigraphy: an integrated approach. Elsevier Science B.V., Amsterdam, p. 315–341.

Di Stefano, A., 1995. Biostratigrafia a nannofossili calcarei dei sedimenti medio-supramiocenici del settore occidentale del Plateau Ibleo (Sicilia Sud-Orientale). Bollettino della Società Paleontologica Italiana **34**(2), 147–162.

Di Stefano, A., Foresi, L.M., Lirer, F., Iaccarino, S.M., Turco, E., Amore, F.O., Mazzei, R., Morabito, S., Salvatorini, G., Abdul Aziz, H., 2008. Calcareous plankton high resolution bio-magnetostratigraphy for the Langhian of the Mediterranean area. Rivista Italiana di Paleontologia e Stratigrafia **114**, 51–76.

Di Stefano, A., Verducci, M., Cascella, A., Iaccarino, S.M., 2011a. Calcareous plankton events at the Early/Middle Miocene transition of DSDP Hole 608: comparison with Mediterranean successions for the definition of the Langhian GSSP. Stratigraphy **8**(2–3), 145–161.

Di Stefano, A., Verducci, M., Maniscalco, R., Speranza, F., Foresi, L.M., 2011b. High-resolution stratigraphy of the Contrada Pesciarello borehole succession (SE Sicily): a

Uncorrected Proofs

lower Langhian reference section for the Mediterranean region. Stratigraphy **8**(2–3), 111–124.

Fisher, R.A., 1953. Dispersion on a sphere. Proceedings of the Royal Society of London **217**, 295–305.

Foresi, L.M., Baldassini, N., Sagnotti, L., Lirer, F., Di Stefano, A., Caricchi C., Verducci, M., Salvatorini, G., Mazzei, R., 2014. Integrated stratigraphy of the St.Thomas section (Malta Island): a reference section for the lower Burdigalian of the Mediterranean Region. Marine Micropaleontology **111**, 66–89.

Foresi, L.M., Bonomo, S., Caruso, A., Di Stefano, E., Salvatorini, G., Sprovieri, R., 2002. Calcareous plankton high resolution biostratigraphy (foraminifera and nannofossils) of the uppermost Langhian–lower Serravallian Ras Il-Pellegrin section (Malta). Rivista Italiana di Paleontologia e Stratigrafia **108**(2), 195–210.

Foresi, L.M., Iaccarino, S.M., Mazzei, R., Salvatorini, G., Bambini, A.M., 2001. Il plancton calcareo (foraminiferi e nannofossili) del Miocene delle Isole Tremiti. Paleontographia Italica **88**, 1–62.

Foresi, L.M., Verducci, M., Baldassini, N., Lirer, F., Mazzei, R., Salvatorini, G., Ferraro, G., Da Prato, S., 2011. Integrated stratigraphy of St.Peter's Pool section (Malta): new age for the Upper *Globigerina* Limestone member and progress towards the Langhian GSSP. Stratigraphy **8**(2–3), 125–143.

Fornaciari, E., Di Stefano, A., Rio, D., Negri, A., 1996. Middle Miocene quantitative calcareous nannofossil biostratigraphy in the Mediterranean region. Micropaleontology 42, 37–63.

Fornaciari, E., Rio, D., 1996. Latest Oligocene to early middle Miocene quantitative calcareous nannofossil biostratigraphy in the Mediterranean region. Micropaleontology **42**, 1–36.

Garecka, M., 2005. Calcareous nannoplankton from the Podhale Flysch (Oligocene–Miocene, Inner Carpathians, Poland). Methods and Applications in Micropaleontology **124**, 353–369.

Gartner, S., 1992. Miocene nannofossil chronology in the North Atlantic, DSDP Site 608. Marine Micropaleontology **18**(4), 307–331.

Guerrera, F., Tramontana, M., Donatelli, U., Serrano, F., 2012. Space/time tectono-sedimentary evolution of the Umbria-Romagna-Marche Miocene Basin (Northern Apennine, Italy): a foredeep model. Swiss Journal of Geosciences **105**, 325–341.

Hakyemez, A., Toker, V., 2010. Planktonic foraminiferal biostratigraphy from the sedimentary cover of Troodos Massif, Northern Cyprus: Remarks on Aquitanian-Langhian biozonation. Stratigraphy **7**(1), 33–59.

Haq, B.U., Lohman, G.P., 1976. Early Cenozoic nannoplankton biogeography of the Atlantic Ocean. Marine Micropaleontology **1**, 119–194.

Hilgen, F.J., Abels, H.A., Iaccarino, S.M., Krijgsman, W., Raffi, I., Sprovieri, R., Turco, E., Zachariasse, W.J., 2009. The Global Stratotype Section and Point (GSSP) of the Serravallian Stage (Middle Miocene). Episodes **32**, 152–166.

Holkova, K., 2013. Morphological variability of the Paratethyan Oligocene-Miocene small reticulofenestrid coccolites and its paleoecological and paleogeographical implications. Acta Paleontologica Polonica **58**(3), 651–668.

Iaccarino, S.M., 1985. Mediterranean Miocene and Pliocene planktic Foraminifera. In: Bolli, H.M., Saunders, J.B., Perch-Nielsen, K. (Eds.), Plankton Stratigraphy. Cambridge University Press, New York, p.283–314.

Iaccarino, S.M., Di Stefano, A., Foresi, L.M., Turco, E., Baldassini, N., Cascella, A., Da Prato, S., Ferraro, L., Gennari, R., Hilgen, F.J., Lirer, F., Maniscalco, R., Mazzei, R., Riforgiato, F., Russo, B., Sagnotti, L., Salvatorini, G., Speranza, F., Verducci, M., 2011. High-resolution integrated stratigraphy of the Mediterranean Langhian: Comparison with the historical stratotype and new perspectives for the GSSP. Stratigraphy **8**(2–3), 199–215.

Iaccarino, S.M., Premoli Silva, I., Biolzi, M., Foresi L.M., Lirer, F., Turco, E., Petrizzo, M.R., 2007. Practical manual of Neogene planktonic foraminifera. In: Biolzi, M., Iaccarino, S.M., Turco, E., Checconi, A., Rettori, R. (Eds.), International School on Planktonic Foraminifera, (Neogene Planktonic Foraminifera). Perugia, Italy, 141 p.

Iaccarino, S.M., Salvatorini, G., 1982. A framework of planktonic foraminiferal biostratigraphy for early Miocene to Late Pliocene Mediterranean area. Paleontologia Stratigrafica ed Evoluzione **2**, 115–125.

Kennett, J.P., Srinivasan, M.S., 1983. Neogene Planktonic Foraminifera: A Phylogenetic Atlas. Hutchinson Ross Publishing Company, Stroudsburg, Pennsylvania (USA), 265 p.

Kirschvink, J.L., 1980. The least-squares line and plane and the analysis of palaeomagnetic data. Geophysical Journal of the Royal Astronomical Society **62**, 699–718.

Krijgsman, W., Kent, D.V., 2004. Non-uniform occurrence of short-term polarity fluctuations in the Geomagnetic Field? New results from Middle to Late Miocene sediments of the North Atlantic (DSDP Site 608). In: Channell, E.T., Kent, D.V., Lowrie, W., Meert, J.G. (Eds.), Timescales of the Paleomagnetic Field. Geophysical Monograph Series 145, American Geophysical Union, p.161–174.

Lirer, F., Cascella, A., Cesarano, M., Casciello, E., Pappone, G., 2007. Micropaleontological study of the Miocene calcareous turbidite deposits of the Faeto and Tufillo formations (Eastern sector of the Southern Apennines chain). Rivista Italiana di Paleontologia e Stratigrafia **113**(2), 269–286.

Lirer, F., Iaccarino, S.M., 2005. Integrated stratigraphy (cyclostratigraphy and biochronology) of late Middle Miocene deposits in the Mediterranean area and comparison with the North and Equatorial Atlantic Oceans: synthesis of the major results. Terra Nova **17**, 338–349.

Lourens, L.J., Hilgen, F.J., Shackleton, N.J., Laskar, J., Wilson, D., 2004. The Neogene Period. In: Gradstein, F.M., Ogg, J.G., Smith, A.G. (Eds.), A Geologic Time Scale 2004. Cambridge University Press, Cambridge, p.409–430.

McFadden, P.L., 1990. A new fold test for paleomagnetic studies, Geophysical Journal International **103**, 163–169.

McFadden, P.L., McElhinny, M.W., 1990. Classification of the reversal test in paleomagnetism. Geophysical Journal International **130**, 725–729.

Uncorrected Proofs

Makrodimitras, G., Stoykova, K., Vakalas, I., Zelilidis, A., 2010. Age determination and paleogeographic reconstruction of Diaponida Islands in NW Greece, based on calcareous nannofossils. Bulletin of the Geological Society of Greece 43(2), 675–684.

Mancin, N., Pirini, C., Bicchi, E., Ferrero, E., Valleri, G., 2003. Middle Eocene to middle Miocene planktonic foraminiferal biostratigraphy for internal basins (Monferrato and Northern Apennines, Italy). Micropaleontology **49**, 341–358.

Martini, E., 1971. Standard Tertiary and Quaternary calcareous nannoplankton zonation. In: Farinacci, A., (Eds.), Proceedings of 2nd International Conference on Planktonic Microfossils, Rome, Italy, 1970, p. 739–785.

Marunteanu, M., 1999. Litho- and biostratigraphy (calcareous nannoplankton) of the Miocene deposits from the outer Moldavides. Geologica Carpathica **50**(4), 313–324.

Miller, K.G., Feigenson, M.D., Wright, J., Bradford, C.M., 1991. Miocene isotope reference section, Deep Sea Drilling Project Site 608: an evaluation of isotope and biostratigraphic resolution. Paleoceanography **6**(1), 33–52.

Montanari, A., Bice, D.M., Capo, R., Coccioni, R., Deino, A., De Paolo, D.J., Emmanuel, L., Monechi, S., Renard, M., Zevenboom, D., 1997. Integrated stratigraphy of the Chattian to mid-Burdigalian pelagic sequence of the Contessa Valley (Gubbio, Italy). In: Montanari, A., Odin, G.S., Coccioni, R. (Eds.), Miocene Stratigraphy: an integrated approach. Elsevier Science B.V., Amsterdam, p. 249–277.

Mourik, A.A., Abels, H.A., Hilgen, F.J., Di Stefano, A., Zachariasse, W.J., 2011. Improved astronomical age constraints for the Middle Miocene climate transition based on high-resolution stable isotope records from the central Mediterranean Maltese Island. Paleoceanography 26, PA1210. doi:10.1029/2010PA001981

Okada, H., Bukry, D., 1980. Supplementary modification and introduction of code numbers to the low latitude coccolith biostratigraphy zonation. Marine Micropaleontology **51**, 321–325.

Olafsson, G., 1991. Quantitative calcareous nannofossils biostratigraphy and biochronology of Early through Late Miocene sediments from DSDP Hole 608. Meddelanden från Stockholm Universitets Institution för Geologi och Geokemi **203**, 1–28.

Postuma, J.A., 1971. Manual of planktonic foraminifera. Amsterdam, Elsevier Publishing Company, 420 p.

Raffi, I., Backman, J., Fornaciari, E., Pälike, H., Rio, D., Lourens, L., Hilgen, F., 2006. A review of calcareous nannofossil astrobiochronology encompassing the past 25 million years. Quaternary Science Reviews **25**, 3113–3137.

Rio, D., Raffi, I., Villa, G., 1990. Pliocene–Pleistocene calcareous nannofossil distribution patterns in the Western Mediterranean. In: Kastens, K.A., Mascle, J. et al. (Eds.), Proceedings of the Ocean Drilling Program, Scientific Results 107 (College Station, TX), p. 513–533.

Rögl, F., Nagymarosy, A., 2004. Biostratigraphy and correlation of the Lower Miocene Michelstetten and Ernstbrunn sections in the Waschberg Unit, Austria (Upper Egerian to Eggenburgian, Central Paratethys). Courier Forschungsinstitut Senckenberg **246**, 129–151.

Ruddiman, W.F., Kidd, R.B., Thomas, E. et al., 1987. Site 608. In: Ruddiman, W.F. et al. (Eds.), Initial Reports of the Deep Sea Drilling Project 94, Washington DC: Government Printing Office, p. 149–246.

Salvatorini, G., Cita, M.B., 1979. Miocene foraminiferal stratigraphy, DSDP Site 397 (Cape Bojador, North Atlantic). In: Ryan, W.B.F. et al. (Eds.), Initial Reports of the Deep Sea Drilling Project, **47**(1), p. 317–373.

Shackleton, N.J., Crowhurst, S.J., Weedon, G.P., Laskar, J., 1999. Astronomical calibration of Oligocene–Miocene time. Philosophical Transactions of the Royal Society of London Series A – Mathematical Physical and Engineering Sciences **357**, 1907–1929.

Speranza, F., Sagnotti, L., Mattei, M., 1997. Tectonics of the Umbria–Marche-Romagna Arc (central northern Apennines, Italy): New paleomagnetic constraints. Journal of Geophysical Research **102**, 3153–3166.

Spezzaferri, S., 1994. Planktonic foraminiferal biostratigraphy and taxonomy of the Oligocene and lower Miocene in the oceanic record. An overview. Paleontographia Italica **81**, 1–187.

Spezzaferri, S., 1996. Paleoclimatic interpretations of the late Oligocene-early Miocene planktonic foraminiferal record from the Lemme-Carrosio Section (Northern Italy). Giornale di Geologia **581**(1–2), 119–139.

Sprovieri, R., Bonomo, S., Caruso, A., Di Stefano, A., Di Stefano, E., Foresi, L.M., Iaccarino, S.M., Lirer, F., Mazzei, R., Salvatorini, G., 2002. An integrated calcareous plankton biostratigraphic scheme and biochronology for the Mediterranean Middle Miocene. Rivista Italiana di Paleontologia e Stratigrafia **108**(2), 337–353.

Theodoridis, S., 1984. Calcareous nannofossils biozonation of the Miocene and revision of the Helicoliths and *Discoaster*. Utrecht Micropaleontological Bulletins **32**, 1–271.

Turco, E., Cascella, A., Gennari, R., Hilgen, F.J., Iaccarino, S.M., Sagnotti, L., 2011a. Integrated stratigraphy of the La Vedova section (Conero Riviera, Italy) and implications for the Burdigalian/Langhian boundary. Stratigraphy **8**(2–3), 89–110.

Turco, E., Iaccarino, S.M., Foresi, L.M., Salvatorini, G., Riforgiato, F., Verducci, M., 2011b. Revisiting the taxonomy of the intermediate stages in *Globigerinoides – Praeorbulina* lineage. Stratigraphy **8**(2–3), 163–188.

Wade, B.S., Pearson, P.N., Berggren, W.A., Pälike, H., 2011. Review and revision of Cenozoic tropical planktonic foraminiferal biostratigraphy and calibration to the geomagnetic polarity and astronomical time scale. Earth-Science Reviews **104**, 111–142.

Young, J.R., 1998. Neogene. In: Bown, P.R. (Eds.), Nannofossil Biostratigraphy. Chapman and Hall, London, p. 225–265.

Zijderveld, J.D.A., 1967. A.C. demagnetization of rocks: Analysis of results. In: Collinson, D.W., Creer, K.M., Runcorn, S.K. (Eds.), Methods in Palaeomagnetism. Elsevier, New York, p. 254–286.

Manuscript received: February 11, 2014; rev. version accepted: November 12, 2014.

uncorrected proofs